Energy & Environmental Science

ROYAL SOCIETY OF CHEMISTRY

PAPER

View Article Online
View Journal | View Issue

Cite this: *Energy Environ. Sci.*, 2026, **19**, 2028

Scaling green hydrogen and CCUS *via* cement–methanol co-production in China

Yuezhang He,[abc] Hongxi Luo,[b] Yuancheng Lin,[a] Carl J. Talsma,[d] Anna Li,[c] Zhenqian Wang,[ae] Yujuan Fang,[f] Pei Liu, *[a] Jesse D. Jenkins,*[bc] Eric Larson *[b] and Zheng Li*[af]

High costs of green hydrogen and of carbon capture, utilization, and sequestration (CCUS) have hindered policy ambition and slowed real-world deployment, despite their importance for decarbonizing hard-to-abate sectors, including cement and methanol. Given the economic challenges of adopting CCUS in cement and green hydrogen in methanol production separately, we propose a renewable-powered co-production system that couples electrolytic hydrogen and CCUS through molecule exchange. We optimize system configurations using an hourly-resolved, process-based model incorporating operational flexibility, and explore integrated strategies for plant-level deployment and CO_2 source-sink matching across China. We find that co-production could reduce CO_2 abatement costs to \$41–53 per tonne by 2035, significantly lower than approximately \$75 for standalone cement CCUS and over \$120 for standalone renewable-based methanol. Co-production is preferentially deployed at cement plants in renewable-rich regions, potentially reshaping national CO_2 infrastructure planning. This hydrogen–CCUS coupling paradigm could accelerate industrial decarbonization and scaling for other applications.

Received 4th December 2025,
Accepted 3rd February 2026

DOI: 10.1039/d5ee07379k

rsc.li/ees

Broader context

Industrial sectors such as cement and chemicals are central to economic development but account for a growing share of global CO_2 emissions. Green hydrogen and carbon capture, utilization and storage (CCUS) are widely viewed as essential options for deeply decarbonizing these "hard-to-abate" industries, yet their high costs and infrastructure requirements remain major barriers to deployment at scale. New opportunities emerge when green hydrogen production is coupled with oxy-fuel cement kilns and CO_2 capture, so that by-product oxygen and captured CO_2 are reused within an integrated co-production system. Here we show how industrial symbiosis between cement production and methanol synthesis can create bidirectional molecular flows and lower costs. We combine an hourly-resolved plant-level optimization model with CCS source–sink matching to explore system configurations, flexible operation under variable renewable electricity, and plant-by-plant deployment pathways for China's cement fleet. Our results show that co-producing clinker and green methanol cuts costs significantly relative to decarbonizing cement and methanol separately, while reshaping the national CO_2 network. Beyond this specific case, the framework shows how coupling hydrogen, CO_2 and O_2 flows across sectors can inform infrastructure planning and circular-economy policy for industrial decarbonization.

1. Introduction

Delivering on global climate targets requires rapid and far-reaching emissions reductions across all sectors, including heavy industries.[1] Green hydrogen and CCUS are widely regarded as indispensable for decarbonizing sectors such as steel, cement, and chemicals, where fossil feedstocks, high-temperature heat, and process-related carbon dioxide (CO_2) emissions limit the effectiveness of electrification and efficiency improvements.[2,3] In response, governments have announced increasingly ambitious policy targets, such as the EU's goal of producing 10 Mt of renewable hydrogen and building 50 Mt of CO_2 injection capacity annually by 2030.[4,5] However, real-world progress falls short of

[a] *State Key Lab of Power Systems, Department of Energy and Power Engineering, Tsinghua University, Beijing, China. E-mail: liu_pei@tsinghua.edu.cn, lz-dte@tsinghua.edu.cn*
[b] *Andlinger Center for Energy and the Environment, Princeton University, Princeton, NJ, USA. E-mail: jessejenkins@princeton.edu, elarson@princeton.edu*
[c] *Department of Mechanical and Aerospace Engineering, Princeton University, Princeton, NJ, USA*
[d] *Carbon Solutions LLC, Bloomington, IN 47401, USA*
[e] *Research Institute of Petroleum Processing, Sinopec Corporation, Beijing, China*
[f] *Laboratory of Low Carbon Energy, Tsinghua University, Beijing, China*

expectations and remains far from what net-zero pathways require due to high costs, infrastructure gaps, and uncertain market incentives.[6,7]

Identifying and scaling early applications of electrolytic hydrogen and CCUS that are both economically viable and replicable can accelerate technological learning and enable broader adoption. One promising approach is to exploit industrial symbiosis, where distinct industrial processes are linked by exchange of mass and/or energy for mutual benefit.[8] Existing forms can improve resource efficiency, lower costs, and reduce emissions, as illustrated by cogeneration of heat and power,[9] utilization of petroleum coke for aluminum anodes[10] and substitution of cement clinker with steel slag.[11] However, many of these have limited potential because they serve niche markets or operate only in highly specialized contexts. Symbiotic coupling of electrolytic hydrogen and CCUS through molecular exchange and process integration, as proposed here, could unlock novel and scalable applications of these decarbonization-enabling technologies. The oxygen (O_2) co-produced from water electrolysis can supply oxy-fuel combustion CCUS systems (*e.g.* high-temperature cement kilns),[12] thereby increasing flue-gas CO_2 concentration and reducing or even eliminating the need for air separation units (ASUs). Meanwhile, the captured CO_2 can serve as a carbon feedstock, which together with electrolytic hydrogen, can be used to synthesize methanol and other hydrocarbon-based chemicals, reducing or eliminating CO_2 transport and sequestration costs. In contrast to the predominantly one-way material or energy flows in most industrial symbiosis, coupling green hydrogen and CCUS could create bidirectional molecular linkages. Symbiotic coupling of cement and methanol production integrated with green hydrogen and CCUS is proposed here as a strategy for decarbonizing those industries while also supporting commercial development of green hydrogen and CCUS technologies.

In 2022, cement and methanol production globally emitted approximately 2.4 Gt CO_2[13] and 0.26 Gt CO_2,[14] respectively, together accounting for around 7% of energy related emissions globally. China accounted for 57% of cement and 37% of the methanol production (2020),[15,16] with a large share of carbon-intensive coal-based routes. For cement, efficiency improvements, clinker substitution, and fuel switching can reduce fossil energy use, but roughly two thirds of emissions are from carbonate calcination and essentially unavoidable without capture, which makes CCUS indispensable.[17] For methanol, dependence on fossil derived hydrogen and carbon feedstocks means that deep reductions require cleaner inputs, such as renewable hydrogen and carbon neutral CO_2 from biogenic sources or direct air capture.[18,19] China is already piloting cement CCUS using oxy-fuel combustion[20] and renewable hydrogen-based methanol projects that source CO_2 from biomass or industrial flue gas.[21,22] However, standalone deployment of CCUS in cement and renewable hydrogen-based methanol remain expensive. Equipment level improvements in cement capture systems and plant level source–sink optimization can reduce capture, transport and storage costs.[23,24] Renewable methanol pathways that pair electrolytic hydrogen with direct air capture and operational flexibility can lower levelized costs.[25,26] Yet, the green premium is estimated at over 40% for cement and more than 100% for methanol compared to conventional pathways.[26,27]

Linking cement and methanol, two historically unconnected sectors, through green hydrogen and CCUS could reduce green premiums for both. Previous studies on methanol production explored clinker kiln off-gases as a carbon source, including using captured CO_2 for catalytic hydrogenation with renewable hydrogen,[19] employing electrochemical CO_2 reduction,[28] and reforming flue gases with natural gas.[29] For cement, prior work on cement oxy-fuel combustion evaluated the benefits of utilizing byproduct O_2 from water electrolysis to replace O_2 from ASU.[30] Our previous work proposed a co-located configuration that enables bidirectional exchange of O_2 and CO_2 between cement kilns and methanol synthesis units.[31] We found synergistic economic and environmental benefits for both sectors and estimated that such co-production routes could account for 24% of China's clinker output and 55% of its methanol production by 2060. Despite these promising findings, two critical aspects of the co-production system warrant deeper investigation.

One is flexibility of operations. Traditionally, industrial facilities have been designed for continuous operation, relying on stable fossil energy supplies to maximize utilization and economic performance. Integrating variable renewable energy introduces variability and intermittency that require storage and flexible operation across units and time scales.[32,33] In the co-production system, multiple process streams and interlinked energy and material flows create a complex, tightly coupled multi-vector topology, calling for a unified optimization modeling framework that captures cross commodity flexibility and interdependent storage dynamics.

The second is facility-level deployment and system-level planning. The economic viability of co-production hinges on renewable quality and on proximity to CO_2 sequestration sites. Spatial heterogeneity in wind, solar and sequestration availability thus mandates a two-tiered approach: plant-specific techno-economic analysis using high-resolution renewable profiles, coupled with system-level geospatial CO_2 pipeline and storage network optimization to identify least-cost clusters for co-production roll-out.

In the present work, we develop a detailed process-based and hourly-resolved model that incorporates unit level flexibility under solar and wind supply and explicitly manages flows of H_2, O_2 and CO_2, as shown in Fig. 1. We represent the entire supply and utilization chain of commodities within the co-production system of cement fueled by biomass and methanol synthesized from green H_2 and captured CO_2, covering production, storage (in different states), consumption, and sequestration (if applicable), as shown in Fig. 7 (see Appendix). Then, we optimize capacity sizing, flexible operation, and storage across different cement-to-methanol stoichiometries (see Table 1). We conduct plant-level analysis of existing cement plants to evaluate the cost-effectiveness and spatial heterogeneity of

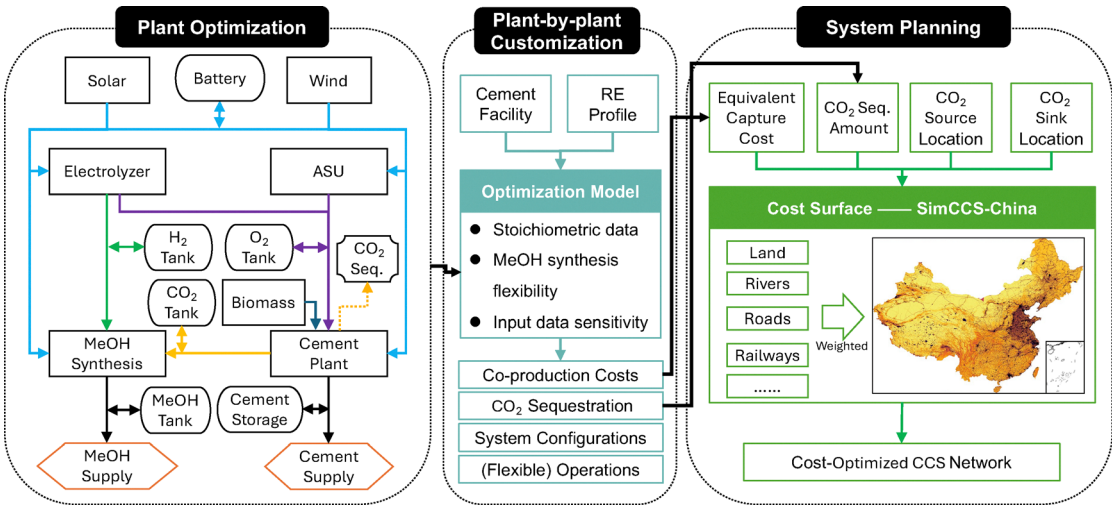

Fig. 1 Schematic diagram of the methodological framework.

Table 1 Scenario settings for cement–methanol system decarbonization. CO_2 emission reduction is defined as the proportion of CO_2 emissions avoided relative to incumbent coal-based technologies, specifically for the case where methanol is used as a shipping fuel. The accounting scope includes direct CO_2 emissions from cement and methanol production and direct CO_2 emissions from methanol combustion, assuming complete combustion. In the net-zero cement & methanol scenario, all process and uncaptured CO_2 emissions are fully balanced by geological sequestration, and the carbon embodied in methanol is entirely atmosphere-neutral, so that net CO_2 released into the atmosphere is zero within our accounting boundary (see details in Section 3 in the SI)

Scenario	CO_2 handling strategy	Cement-to-methanol stoichiometry	CO_2 emission reduction (%)	Methanol synthesis flexibility	Notes
Net-zero cement & methanol	Partial CO_2 sequestration allowed	9.76	100%	Flexible Inflexible	Aligned with certification schemes (*e.g.*, ISCC sustainable marine fuels) that require methanol to use biogenic or atmospheric CO_2 for long-term shipping fuel eligibility
No-CO_2 sequestration	All captured CO_2 used for methanol synthesis	2.77	84%	Flexible Inflexible	Represents a closed-loop carbon pathway; no geological sequestration is allowed
Separate decarbonization	Cement and methanol decarbonized independently	9.76 2.77	77% 89%	Flexible	Cement with standalone CCUS; methanol produced *via* standalone green H_2 and CO_2 sourced from DAC

technology deployment. We integrate the process optimization model with a SimCCS-China model[34] to optimize CO_2 source–sink matching considering costs of pipeline construction across China. This enables generating comprehensive deployment strategies of co-production technologies under different CO_2 sequestration scenarios. We find that this co-production system could achieve a much lower overall abatement cost than decarbonizing these two sectors separately, primarily benefiting from more economical sources of O_2 and CO_2. Unlocking the flexibility of methanol synthesis and configuring molecular storage buffers offer additional but plant-specific economic benefits compared to steady and continuous production. Additionally, introducing co-production technology could have a significant impact on CO_2 transport network planning in China's cement industry, by prioritizing CCS implementation at cement facilities with abundant proximate renewable resources.

2. Results

2.1. Co-production reduces CO_2 abatement costs by lowering supply costs of O_2 and CO_2

We find that the co-production system can achieve a 38–65% reduction in CO_2 abatement costs compared to decarbonizing the two plants separately when considering a selected case-study facility in Inner Mongolia (Fig. 2a). Despite slightly higher H_2 costs (Fig. 2b), the cost savings primarily stem from lower-cost O_2 (Fig. 2c) and CO_2 (Fig. 2d). The increase in H_2 costs arises because O_2 consumption and CO_2 generation in cement kiln introduce inflexible elements to the system, limiting the ability of H_2 production to follow renewable availability as flexibly as in standalone H_2-based methanol. By diminishing the ASU, the system lowers both capital investment and energy consumption, resulting in a 71–95% decrease in O_2 costs (Fig. 2c). However, due to the temporal mismatch between variable O_2 production and fixed O_2 consumption, O_2 storage

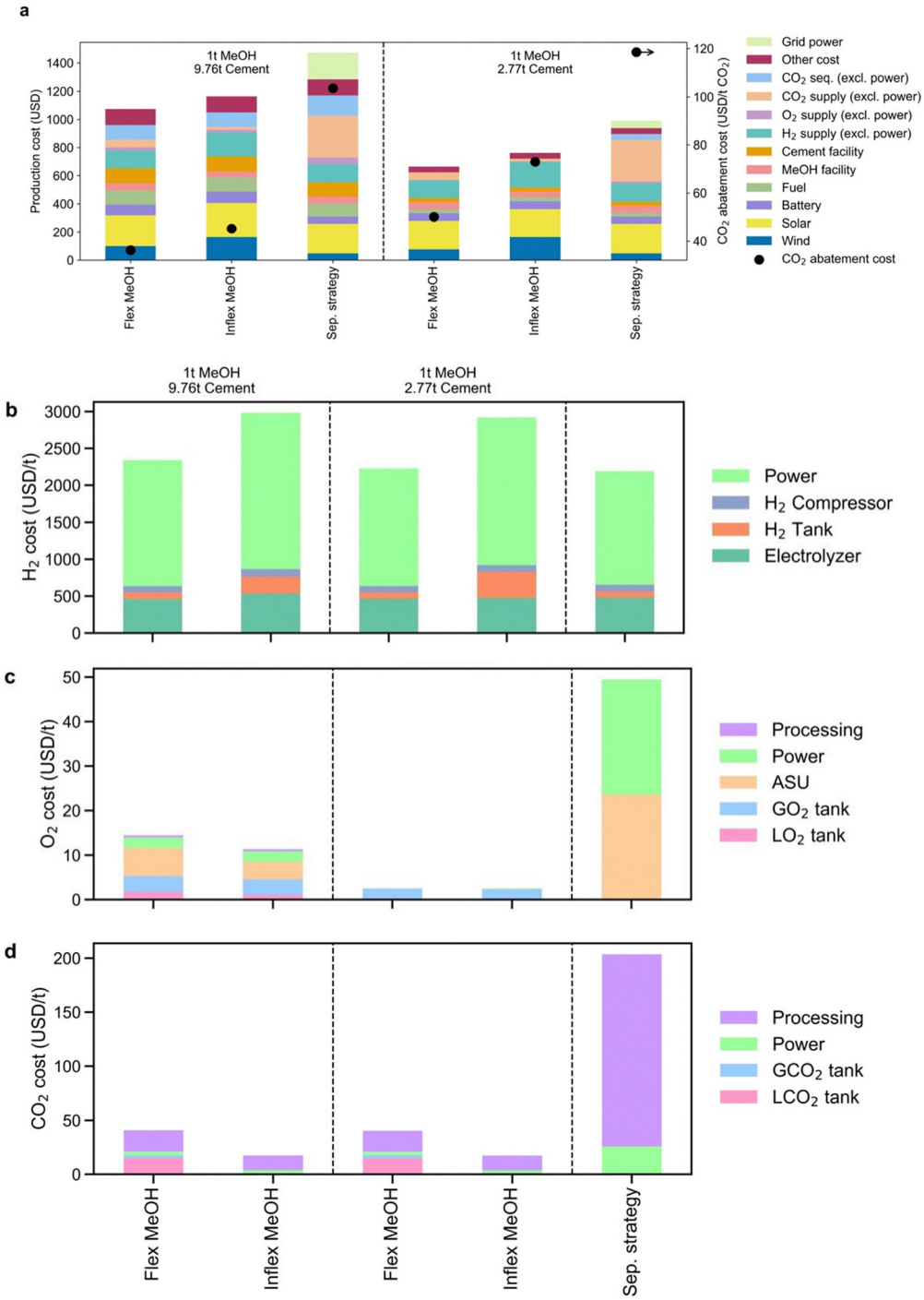

Fig. 2 Cost structure of the co-production system and associated molecules for the selected plant in Inner Mongolia. (a) Cost breakdown of the co-production technology. CO_2 abatement cost is defined as the cost difference between the decarbonized technology and the incumbent dominant route without emissions abatement (*i.e.*, coal-based production and current grid electricity), divided by the corresponding emission reduction. In this case study, the CO_2 abatement cost for separate decarbonization is estimated at \$79 per tonne of CO_2 for cement and \$131 per tonne of CO_2 for methanol (see Section 3 in the SI for detailed calculations). The CO_2 abatement cost presented in this figure reflects the combined cost for cement and methanol under a given stoichiometric ratio. "Other costs" include labor and miscellaneous cement raw materials. "CO_2 seq." represents the costs associated with CO_2 compression, transport and sequestration, assuming the transport cost is \$8.7 per tCO_2 and storage cost is \$5.8 per tCO_2.[35] (b), cost breakdown of H_2 supply. (c) Cost breakdown of O_2 supply. (d) Cost breakdown of CO_2 supply. "Processing" in (c) and (d) refers to capital and operational costs associated with compressors (for gaseous storage) and liquefaction units (for liquid storage).

and its associated processes constitute the largest share of the O_2 cost structure. In the no-CO_2 sequestration scenario, the amount of byproduct O_2 is 2.7 times the O_2 demand, eliminating the necessity for O_2 storage tanks. Capturing, processing and

storing CO_2 from cement production is 80–91% cheaper than costs of CO_2 from DAC, as shown in Fig. 2d. We use a relatively optimistic DAC cost at \$203.6 per tCO_2,[26] within the typical \$200–600 per tCO_2 range (see Section 3 in the SI for the literature review on DAC). Applying partial CO_2 sequestration could reduce CO_2 abatement costs by further leveraging the economically sourced O_2.

Also, unlocking the flexible operation of methanol synthesis could reduce overall production costs by 8–12% primarily due to lower H_2 costs, despite slight increases in O_2 and CO_2 costs. Harnessing demand-side flexibility in H_2 consumption can reduce the levelized cost of electricity (LCOE) from solar and wind sources and the required H_2 storage tank size, ultimately lowering the levelized cost of hydrogen (LCOH) by 22–24% (Fig. 2b). Inflexible methanol synthesis requires a stable, hour-by-hour supply of CO_2 and H_2. The fixed CO_2 extraction from clinker kilns aligns perfectly with the stable CO_2 demand, eliminating the need for CO_2 storage tanks. However, with flexible methanol synthesis scenarios, the flexible CO_2 demand and stable CO_2 supply create operational asynchrony and necessitate CO_2 storage tanks as a buffer. Similarly, O_2 supply is more compatible with a fixed demand, which reduces the cost of O_2 through downsized storage tanks and a smaller complementary ASU. Thus, maximizing the flexibility options could reduce overall system costs, but it requires more coordinated and complex system design and operations.

2.2. Optimized system configurations and flexible operations

By coupling flexibilities across processes, the variability of renewable generation cascades through all production and storage stages, with each component contributing to accommodating renewable fluctuations. We observe distinct patterns of optimal flexible operations across components within the co-production system under the net-zero cement & methanol scenario (Fig. 3). In the case-study plant in Inner Mongolia, electrolyzer loads closely follow the combined generation of solar and wind, operating primarily during the daytime while shutting down or reducing output at night. Methanol synthesis exhibits seasonal variations, operating at full load during most of the spring. Batteries, exhibiting an intra-day cycle, predominantly charge during the daytime and discharge at night. H_2 and gaseous O_2 storage tanks exhibit similar annual charge–discharge cycles, typically ranging from hours to days. Gaseous CO_2 tanks cycle 21 times per year, but with uneven temporal distribution across the year. In contrast, liquid O_2, liquid CO_2, and methanol storage function as long-duration storage, with the number of annual round-trip cycles ranging from 2.1 to 3.9. While liquid O_2 and methanol are charged in spring and summer when renewable generation is abundant and discharged in other periods, liquid CO_2 follows the opposite pattern.

The discrepancy in storage behavior among different commodities can be explained by unit capital cost considerations. Storage technologies with low capital costs per unit of stored volume (*e.g.*, liquid storage) tend to exhibit long-duration storage, despite the high capital and energy penalties associated with charging and discharging, aligning with findings in a previous study.[36] Conversely, storage with higher volume capacity costs (*e.g.*, gaseous storage) is inclined to increase cycling frequency, diluting capital costs across higher turnover rates to improve cost efficiency per unit of stored commodity or energy. Overall, these operational patterns reflect the underlying variability of renewable resources, highlighting that the value of flexibility lies in enabling reliable integration of intermittent solar and wind.

In contrast to RE-rich weeks characterized by nearly full-load methanol synthesis, RE-scarce weeks feature frequent ramping, which drives distinct patterns in H_2, O_2, and CO_2 production, storage, and consumption. We analyze representative RE-scarce and RE-abundant weeks for the plant in Inner Mongolia, focusing on the balance of electricity, H_2, O_2, and CO_2, as shown in Fig. 4. Here, the RE-scarce week is characterized by persistently low renewable output, especially weak nighttime wind availability, whereas the RE-abundant week exhibits consistently higher wind and/or solar. Electrolyzers account for 85% of power consumption annually, with batteries discharging primarily at night to maintain the minimum electrolyzer load (5%). During RE-rich weeks, electrolyzers could operate overnight, powered by strong wind generation. H_2 storage is discharged at night to supplement the minimum H_2 supply required for methanol synthesis. Beyond real-time consumption, most excess O_2 is stored in gaseous form, supplementing demand at night. During RE-scarce weeks, liquid O_2 storage experiences lower charging and higher discharge, while ASU operates at a higher load compared to RE-rich weeks. Meanwhile, some O_2 may be vented in RE-rich weeks, indicating a trade-off between maximizing byproduct O_2 utilization and minimizing O_2 storage system costs. For CO_2 storage, gaseous CO_2 remains largely idle, while liquid CO_2 undergoes net discharge during RE-abundant weeks. Conversely, in RE-scarce weeks, gaseous CO_2 is charged at night and utilized on days with relatively higher renewable output, whereas liquid CO_2 is charged continuously without discharge.

2.3. Geographic differences in plant economic performance due to RE spatial heterogeneity

Given the estimated shrinking cement demand[37,38] and the expanding methanol market[39] in China, we consider a scenario where new methanol facilities are co-located with existing cement plants (823 plants in total). We focus on greenfield methanol facilities because the current methanol fleet is predominantly coal-based and incompatible with low-carbon integration, whereas cement could involve retrofit. In the net-zero cement & methanol scenario (9.76 tonnes cement per tonne methanol), the spatial heterogeneity of renewable resources leads to variations in CO_2 abatement costs (see Fig. 5a, excluding CO_2 transport and sequestration costs) and results in diverse optimized system configurations and operational strategies (see Section 1 in the SI). Cement plants located in Northeast China and North-Central China, where renewable resources are abundant, achieve lower CO_2 abatement costs (excluding CO_2 transport and storage), approximately \$15–35

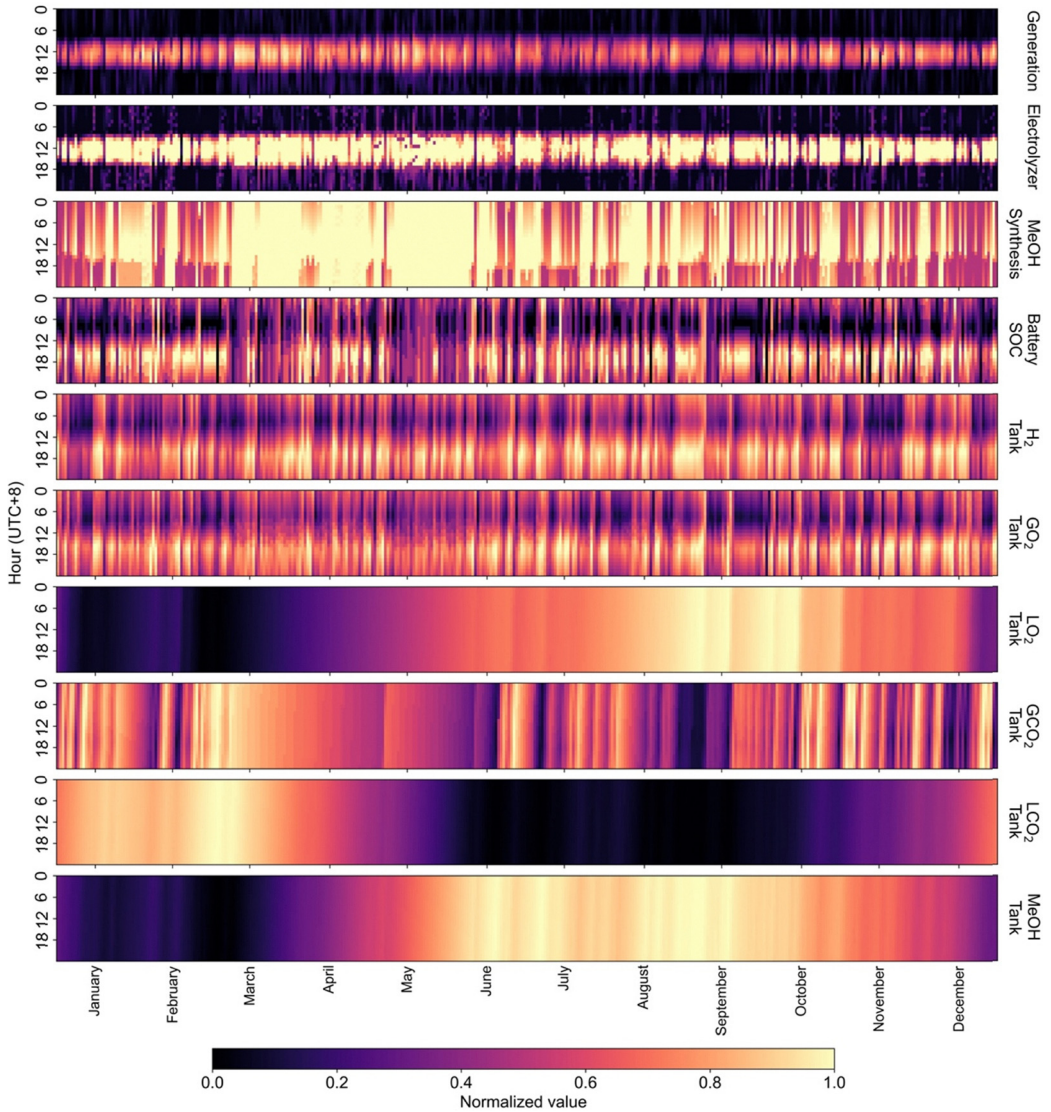

Fig. 3 Annual normalized operational profiles of the selected plant in Inner Mongolia under the net-zero cement & methanol scenario with flexible methanol synthesis. The *x*-axis represents 365 days over one year, and the heat maps illustrate hourly variations, with the *y*-axis indicating 24 hours per day. Values are normalized by dividing hourly absolute values by their annual maximum (linear normalization). "Generation" denotes the actual hourly power generation from solar and wind, normalized by the weather-dependent maximum available hourly generation. "Electrolyzer" and "MeOH synthesis" indicate hourly loads normalized by their respective maximum loads. "State of charge (SOC)" for battery, H_2 tank, gaseous O_2 (GO_2) tank, liquid O_2 (LO_2) tank, gaseous CO_2 (GCO_2) tank, liquid CO_2 (LCO_2) tank, and MeOH tank refer to the hourly SOC normalized by each component's maximum SOC over the entire year. The operations under inflexible methanol synthesis are shown in Fig. 8 (see Appendix).

per metric ton. For example, the case plant in Inner Mongolia falls within this range, with an abatement cost of $31 per metric ton. In contrast, plants located in central China exhibit higher abatement costs, often exceeding $40 per metric ton of CO_2.

Unlocking the flexibility of methanol synthesis yields plant-specific cost reductions, with cement plants in China achieving co-production cost savings ranging from 3% to 17% (Fig. 5b). Generally, plants with lower baseline co-production costs under inflexible methanol synthesis exhibit smaller marginal benefits from adding flexibility. Nevertheless, enabling flexible methanol synthesis can still achieve over $5 per metric ton in CO_2 abatement cost savings for each unit of added capacity following the ascending order of abatement cost (Fig. 5c).

Although CO_2 abatement costs for most plants are more sensitive to solar costs, the lowest-cost plants rely more heavily on high-quality wind resources and are therefore more sensitive to wind costs. For most plants, solar power accounts for a larger share of total system costs, averaging 11% compared with 5% for wind and 4% for electrolyzers. However, for plants with relatively low CO_2 abatement costs, wind cost parameters can emerge as the dominant sensitivity factor. For example, among the 50 lowest-cost plants, wind averages 9% of total costs compared with 6% for solar. These results suggest that while large-scale cost reductions depend on declining solar costs, achieving the lowest abatement costs might require prioritizing deployment in regions with high-quality wind resources.

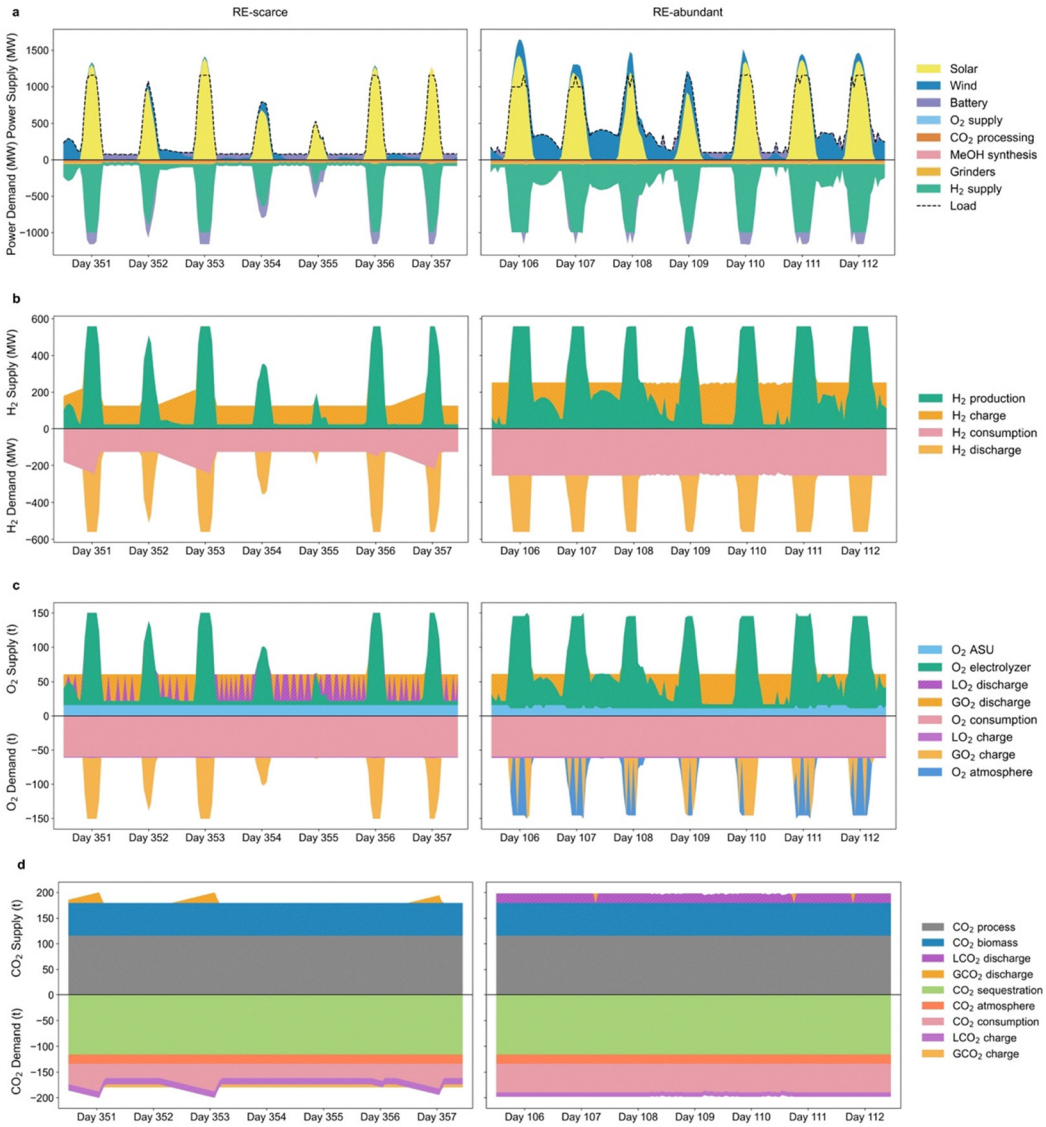

Fig. 4 Operational profiles under renewable energy (RE)-scarce (left panel) and RE-abundant (right panel) weeks for the selected plant in Inner Mongolia under the net-zero cement & methanol scenario with flexible methanol synthesis. Positive values indicate the supply (including discharge) of each commodity, while negative values indicate demand (including charge). (a) Electricity balance. The dashed line indicates the aggregated electricity load; power generation exceeding the load is curtailed. "O_2 supply" includes electricity consumed by the ASU, compressors, and liquefaction units. "CO_2 processing" includes electricity consumed by compressors and liquefaction units. "H_2 supply" represents electricity consumption for water electrolysis and H_2 compression. (b) H_2 balance. (c) O_2 balance; "O_2 atmosphere" indicates vented O_2. (d) CO_2 balance; "CO_2 process" indicates CO_2 from carbonate decomposition, "CO_2 biogenic" indicates CO_2 from biomass combustion, and "CO_2 atmosphere" refers to CO_2 emitted to the atmosphere due to a less than 100% capture rate. The operations under inflexible methanol synthesis are shown in Fig. 9 (see Appendix).

2.4. Effect of co-production on planning of CO_2 source–sink matching

Although the abovementioned optimization model evaluates the economic performance based on renewable resource availability, incorporating post-capture (*i.e.*, transportation and storage) costs may alter the overall production cost distribution and influence the optimal plant selection strategy. Consequently, a co-optimization approach that integrates production and post-capture costs provides insights into the most cost-effective deployment of co-production facilities. To address this, we employ an extended version of SimCCS-China to co-optimize onsite production costs, CO_2 pipeline network design, and CO_2 storage costs under different CO_2 sequestration amount scenarios (see the Methods section and Section 6 in the SI for details). As shown in Fig. 6a and Fig. S38a, the selected cement plants largely align with plants that have lower production costs shown in Fig. 5a. The "CO_2 sequestration 26.0 Mt per year" scenario corresponds to 7.06 Mt per year of methanol output under co-production, while the "CO_2 sequestration 311.5 Mt per year" scenario corresponds to 84.7 Mt per year. At the initial-deployment stage, the low-hanging fruit for adopting co-production technologies is found in Northeast

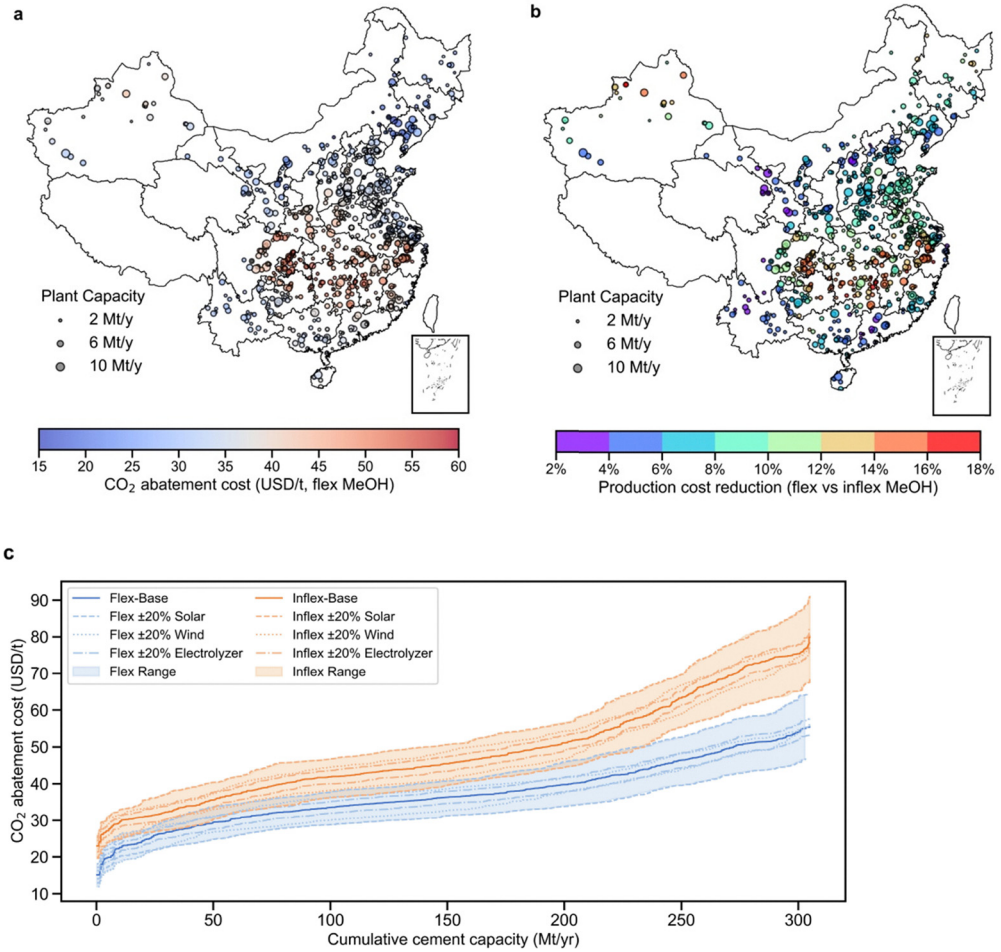

Fig. 5 Plant-by-plant economic performance and sensitivity analysis in China under net-zero cement & methanol scenarios. (a) CO_2 abatement cost by plant, defined as ($cost_{decarbonized} - cost_{incumbent}$) /$\Delta CO_2$ per 9.76 t cement + 1 t MeOH. Incumbent routes use coal-based production and current grid electricity; CO_2 transport and sequestration costs are excluded. Each dot marks an existing cement plant with a different capacity (size) and abatement cost (color). (b), The ratio of cost difference between flexible (Flex) and inflexible (Inflex) methanol synthesis, on the same 9.76 t cement + 1 t MeOH basis. (c) Cost–capacity curves sorted in ascending order of abatement cost *versus* cumulative cement capacity. The solid blue line is the Flex baseline; lighter blue lines show sensitivity to renewable-related cost parameters under Flex scenarios; the light blue shaded band is the Flex envelope (min–max). The sensitivity analysis is conducted by changing the cost parameters of solar, wind and electrolyzer by 20% one at a time. The solid orange line is the Inflex baseline; lighter orange lines show sensitivity of Inflex; the light orange shaded band is the Inflex envelope. It is assumed that local biomass resources are sufficient to meet the demand under the net-zero cement & methanol scenario, with supporting estimates and an availability analysis provided in Section 4 in the SI.

China, where the additional costs from CO_2 transport and sequestration are approximately $15 per tonne. As CO_2 sequestration increases to large-scale deployment, CO_2 captured from some cement plants in North China, Northeast China, Southwest China, and East China is transported to nearby sequestration sites through a CO_2 pipeline network. However, compared to the plant distribution shown in Fig. 5a, some plants with low production costs are not connected to the network due to their long distances to suitable storage sites.

Meanwhile, the introduction of the co-production system significantly alters the CO_2 source–sink matching layout compared to decarbonizing China's cement sector alone (Fig. 6b and Fig. S38b). Under a cement-only decarbonization strategy, CO_2 pipelines connect fewer plants located in renewable-rich regions such as North China and Northeast China, but with potential expansions into central China. CO_2 transport costs are higher when using co-production technologies, driven by lower capturable CO_2 volumes per plant and more pipeline installations required (Fig. 6c). This indicates that producing net-zero methanol through co-production systems involves a cost trade-off, where increased CO_2 transport requirements are offset by lower production-side abatement costs.

3. Discussion

Co-production, as proposed in this study provides substantial economic advantages over separate decarbonization of the cement and methanol sectors. By 2035, co-producing net-zero cement and methanol in China could lower CO_2 abatement

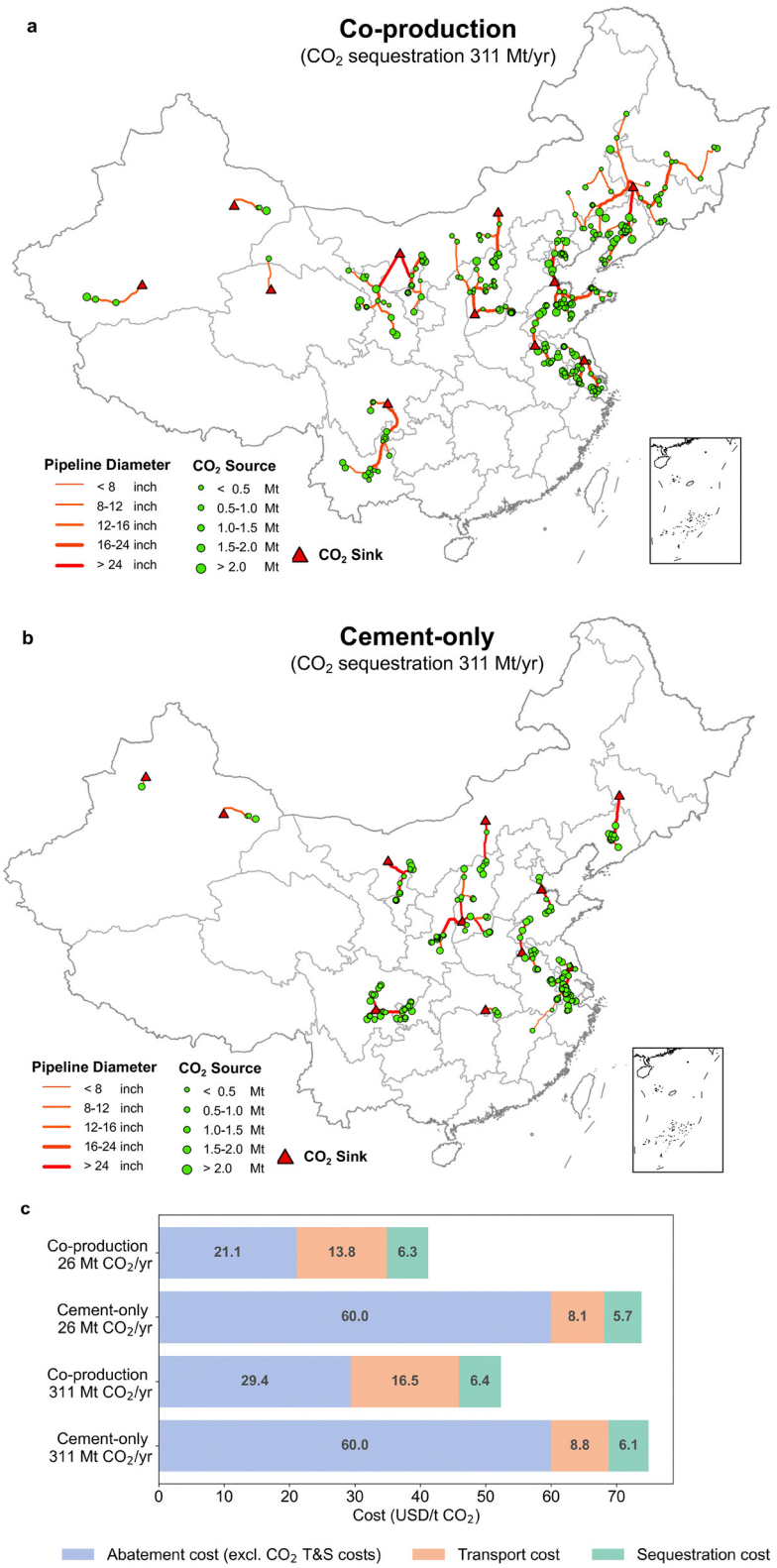

Fig. 6 Comparison of CO_2 source–sink matching under co-production *versus* cement-only decarbonization scenarios. (a) CO_2 network under co-production. (b) CO_2 network under cement-only. (c) The composition of CO_2 abatement costs under different scenarios. Compared to the case-study plant in Inner Mongolia, here we change the CO_2 transport and sequestration costs from fixed value per tonne of CO_2 into variable numbers (see the Methods section). "CO_2 sequestration 311 Mt per year" refers to the scenario where all incumbent methanol production (70.6 Mt) and an estimated share of marine fuel demand (14.1 Mt) are substituted with green methanol under co-production. "CO_2 sequestration 26 Mt per year" corresponds to a scenario with a 10% substitution of incumbent methanol production (7.06 Mt) by co-production (see Fig. S38). Green circles mark CO_2 point sources at cement plants, with size representing capturable emission volume; red triangles mark CO_2 storage sinks. Orange lines denote the proposed CO_2 pipeline network with different diameters reflected by line width. Additional CO_2 sequestration scenarios are presented in Section 7 in the SI.

costs to $41–53 per tonne, markedly below approximately $75 for independent CCS in cement and over $120 for independent renewable-based methanol. With China's carbon price projected to reach $30–70 per tCO_2 by 2035,[40] the co-production approach has promise to achieve cost parity with conventional technologies under plausible policy scenarios while achieving co-decarbonization. Spanning from detailed process modeling to system-level planning, this study offers critical insights into cost-effective and feasible decarbonization pathways for these two hard-to-abate sectors through optimized co-production systems.

Such industrial symbiosis reveals a transferable molecule coupling principle that can materially shape the cost and feasibility of integrated decarbonization systems. H_2 has attracted extensive attention for its potential as an industrial feedstock,[41] spurring technoeconomic analyses and lifecycle emission assessments.[42,43] Conversely, the application potential of renewable-sourced O_2 and CO_2 as industrial feedstocks remains underexplored. Currently, industrial O_2 is primarily sourced through energy-intensive air separation for combustion, chemical synthesis, and metallurgy.[44] In a future industrial system deploying large-scale electrolytic hydrogen, high-purity O_2 generated from water electrolysis could be directed for oxy-fuel combustion, improving carbon capture efficiency and enhancing system-wide decarbonization economics by reducing costs associated with air separation.[45] Meanwhile, captured CO_2 can serve as a raw material for chemical synthesis where a carbon source is needed.[46] Using captured CO_2 is significantly more economical than direct air capture and less emission-intensive than conventional coal-based routes. Thus, the generalized co-production paradigm represents an innovative form of industrial symbiosis that integrates oxy-fuel combustion–CCUS with electrolytic hydrogen, opening new frontiers for industrial decarbonization and delivering mutual benefits for traditionally unconnected sectors.

Exploring the flexibility of industrial processes may further lower the costs of low-carbon technologies. Compared with most stable, continuously operated industrial facilities, a unique feature of the renewable-based co-production system is its integration of operational flexibility across different components and storage methods. Under the flexible methanol synthesis scenario, the temporal mismatch of supply and demand is characterized by: (1) H_2: flexible production and flexible consumption; (2) O_2: flexible production and fixed consumption; (3) CO_2: fixed production and flexible consumption. Different storage methods (*e.g.*, liquid *vs.* gaseous storage) operate at varying storage durations, shaped by their economic and technical parameters. The temporal asynchrony of molecular flows arising from renewable energy variability underscores the necessity and complexity of strategically coordinating operational modes and deploying buffering strategies to optimize system-wide adaptability. In practice, however, first-of-a-kind (FOAK) deployment is likely to operate more conservatively than the system-optimal schedules explored here. Flexible electrolysis and gas buffering are comparatively mature and have been demonstrated in industrial settings.[47] By contrast, flexible methanol synthesis remains largely at the early demonstration stage and is likely limited to narrower turndown ranges and slower ramping, given constraints related to catalyst performance, thermal management, and product quality.[48] Meanwhile, flexible operation may increase O&M burdens or accelerate equipment degradation.[49] We therefore interpret the modeled flexibility as an upper bound on integration value. The trade-off between flexibility benefits and operational penalties must be established through staged demonstration and deployment.

Implementing co-production technologies further demands customized deployment strategies to address the spatial heterogeneity of renewable resources, CO_2 pipeline costs, and sequestration site distributions. Our results indicate that optimal system configurations, economic performance, and potential savings from flexibility vary plant by plant, leading to plant-specific optimal operations across different components. Additionally, achieving net-zero emissions requires co-optimization of renewable-based production alongside CO_2 transport and sequestration planning. Compared to cement-only decarbonization, adopting co-production technologies results in different CO_2 pipeline layouts, both for initial-deployment and large-scale CO_2 sequestration scenarios. Given the substantial investments needed for CO_2 pipeline infrastructure, the deployment of co-production technologies must carefully assess the economic viability and technical feasibility of CO_2 network planning, and be coordinated with potential pipelines designed for the cement sector alone.

Introducing co-production technologies could also influence the decommissioning strategy for China's cement production capacity. In 2020, China produced 2395 Mt cement;[50] however, demand has started to decline, driven by a weakened real estate and infrastructure market, and is projected to decrease by 42-79% by 2060.[37,38] Due to overcapacity and future demand decline, the criteria guiding decisions on cement plant retention are likely to prioritize factors such as plant efficiency rankings, availability of surrounding decarbonization resources (*e.g.*, CO_2 sequestration sites, alternative fuels), and regional cement demand.[24,31,51] Co-production technologies might confer strategic advantages to cement plants located in regions with abundant renewable resources or even stimulate the construction of new capacity in these regions through capacity replacement policies. In contrast, China's methanol market remains robust, supported by both conventional chemical demand and emerging applications such as low-carbon fuels.[52] Our analysis suggests that under the scenario of substituting all conventional methanol and methanol shipping fuel forecast in 2050, co-production technologies would necessitate utilizing approximately 41.3% of China's current cement capacity (see Section 7 in the SI). Therefore, dynamic planning of cement plant decommissioning and the incremental co-production deployment should be comprehensively evaluated for optimizing China's long-term decarbonization pathway.

However, successful deployment will require strong financial incentives, targeted policy support for demonstration projects, and coordinated corporate strategies bridging these

traditionally unrelated industries. In practice, co-production typically spans multiple owners and counterparties, including cement and methanol operators, renewable electricity suppliers or offtakers, and CO_2 transport and storage providers. Aligning incentives requires credible valuation of verified emissions reductions and transparent allocation of that value across participating actors. Bankable deployment will therefore depend on robust contracting arrangements, such as long-term renewable electricity procurement and low-carbon methanol offtake, with clear provisions on risk allocation, long-term liability, and revenue sharing. The limitations of this study (see Section 8 of the SI) reflect modeling abstractions on plant heterogeneity, siting feasibility, carbon-accounting scope, downstream logistics (see the estimated delivered-to-port cost in Section 9 of the SI), and technological constraints on alternative-fuel substitution.[53]

Cement–methanol co-production could become increasingly attractive across a wider set of geographies beyond China. Cement and methanol are globally traded, geographically widespread foundation materials, enabling many opportunities for co-location or regional integration. Consistent with our China-wide sensitivity across renewable endowments, a key prerequisite is access to abundant low-cost renewables. Many regions offer wind and solar resources that are comparable to or stronger than China's (*e.g.*, the U.S. Great Plains, Australia, Chile, and parts of the Middle East and North Africa, among others),[54] while biomass-rich regions (*e.g.*, Brazil) may further ease low-carbon heat supply constraints.[55] Projected declines in the costs of wind, solar, and electrolysis energies would further improve the economics in the future. In parallel, policy and market frameworks that monetize emissions reductions are expanding, including carbon pricing (*e.g.*, the EU ETS) and low-carbon fuel standards. For example, the average 2024 secondary market price of the EU ETS was around \$71 per tCO_2e,[56] *versus* approximately \$14 per tCO_2 for China's national ETS allowances.[57] However, national circumstances differ substantially in resource quality, infrastructure, and policy environments, and the quantitative outcomes therefore merit further country-specific assessment.

4. Methods

4.1. Optimization model

The process-detailed linear programming optimization model is designed to optimize capacity sizing, flexible operations, and storage strategies for each system component at an hourly resolution under constraints (see Section 2 in the SI). Electricity is sourced from a combination of dedicated local solar and wind sources. Locally-sourced biomass is used for clinker calcination, ensuring a carbon-neutral energy supply during the cement production stages. Alkaline electrolyzers generate H_2 and O_2 simultaneously with a flexible load. H_2 must be compressed to 150 bar to meet the pressure requirements for chemical production before being used in methanol synthesis or stored in gaseous H_2 tanks. O_2 can be utilized immediately, stored in gaseous form, or liquefied for long-duration storage. Since the operating pressure of clinker kilns ($\sim$1 bar) is lower than the electrolyzer outlet pressure, O_2 can be used without compression. To manage temporal mismatches, O_2 can either undergo compression and be stored in gaseous tanks (lower energy penalty but higher capital cost per mass stored), or be liquefied and stored in liquid tanks (higher energy penalty but lower capital cost per mass stored). While byproduct O_2 utilization for oxy-fuel combustion offers economic benefits, an ASU is also included to supplement O_2 during temporal shortages or when elevating the stoichiometric balance between cement and methanol reduces byproduct O_2 availability. Cement production is divided into three stages: raw meal preparation, clinker production, and cement production. The output commodity of each stage can be easily stored since the solid outputs have simple storage requirements. Raw meal preparation and cement production involve grinding processes powered by renewable electricity and can operate flexibly. However, the clinker kiln must operate steadily due to the stability requirements of chemical reactions at more than 1500 °C.[58] CO_2 emissions from clinker kilns originate from biomass combustion ($\sim$1/3) and carbonate decomposition ($\sim$2/3). Captured CO_2 can be stored in liquid or gaseous form for future use, or compressed and transported for underground sequestration. For immediate consumption or gaseous storage, CO_2 is compressed to 50 bar, while for sequestration, it is compressed to 150 bar. Similar to O_2 storage, CO_2 storage options include gaseous and liquid storage. Methanol is synthesized from green H_2 and captured CO_2 and stored in liquid form. Methanol synthesis has the potential for flexible operation within a certain load range and ramping limits. We assume a fixed hourly supply for both cement and methanol. The resulting optimization problem involves hundreds of thousands of variables and constraints.

4.2. Input data

Technical and economic parameters were derived from the authors' process simulations and data from the literature. We use ASPEN Plus to simulate the detailed production processes for methanol synthesis, and O_2/CO_2 compression and liquefaction systems (Section 5 in the SI). The energy consumption for these processes is extracted from the simulations. Stoichiometric data for other processes are obtained from the literature and summarized in our previous work (see Table S2 in the SI). Flexibility-related parameters, including ramp rates and adjustable load ranges across all components, are also sourced from the literature (see Table S4 in the SI). The costs of renewable generation technologies, batteries, and electrolyzers are customized for China using 2035 projections. Economic data for other facilities are obtained from the literature (see Table S3 in the SI). Renewable energy profiles are sourced from Renewable.ninja, using 2019 weather data. The biomass cost is set at \$80 per tonne (dry matter). Costs are reported in 2020 USD.

4.3. Stoichiometric balance

The stoichiometric balance between cement and methanol is defined as the hourly supply mass ratio of these two products.

The minimum stoichiometric value occurs when all CO_2 from clinker production is directed to methanol synthesis without CO_2 sequestration. As the stoichiometric number increases, higher cement production corresponds to greater O_2 generation and CO_2 utilization. Excess CO_2 is sequestered, and additional O_2 is from otherwise-vented electrolytic O_2 and/or increased O_2 from air separation. A greater proportion of sequestered CO_2 also improves the overall CO_2 removal rate. In the net-zero scenario, the amount of biogenic CO_2 that is sequestered equals the uncaptured CO_2 emissions plus the CO_2 utilized in methanol synthesis, which is ultimately released into the atmosphere. We evaluate various stoichiometric configurations and present the corresponding economic and environmental performance in Fig. 10 (see Appendix).

4.4. Plant-level customization

We obtain plant-level cement facility data[59] and retrieve hourly renewable energy profiles for each plant location. The national average cement-to-clinker ratio is used to estimate the clinker kiln size at each facility. Given that the typical production line capacity ranges from 2500 to 10 000 metric tons of clinker per day, we exclude outliers because erroneously large values exceed the capacity of any existing cement plant in China, while very small plants are unlikely to be prioritized for CCUS deployment. The total selected cement plant capacity is 2976 Mt per year, corresponding to an average capacity utilization rate of 80% in 2020. We assume this capacity utilization rate remains constant in this study to convert capacity size into cement production. Emission factors and energy efficiency per unit output are kept consistent across all facilities. For each plant, we customize facility size and location-specific renewable profiles. These parameters are then used to run the process-detailed optimization model to assess economic performance, commodity output, and CO_2 emissions. At this stage, each plant is optimized independently without considering interactions with other facilities.

4.5. CO_2 source–sink matching

Achieving net-zero cement and methanol production requires sequestering a portion of the captured CO_2. This necessitates building CO_2 transport and storage infrastructure, and calls for an optimization-based approach to match CO_2 sources with nearby sequestration sinks to minimize system costs. Cement plants are widely distributed because the low-value-added cement products are highly sensitive to transportation costs. Suitable CO_2 storage sites, primarily saline aquifers, are concentrated in specific regions. This results in varying CO_2 transport distances for different plants. CO_2 can be transported *via* trucks, ships, or pipelines. This study adopts pipeline transportation due to its advantages in enabling large-scale, long-distance CO_2 transport for onshore applications and relatively low operational emissions.

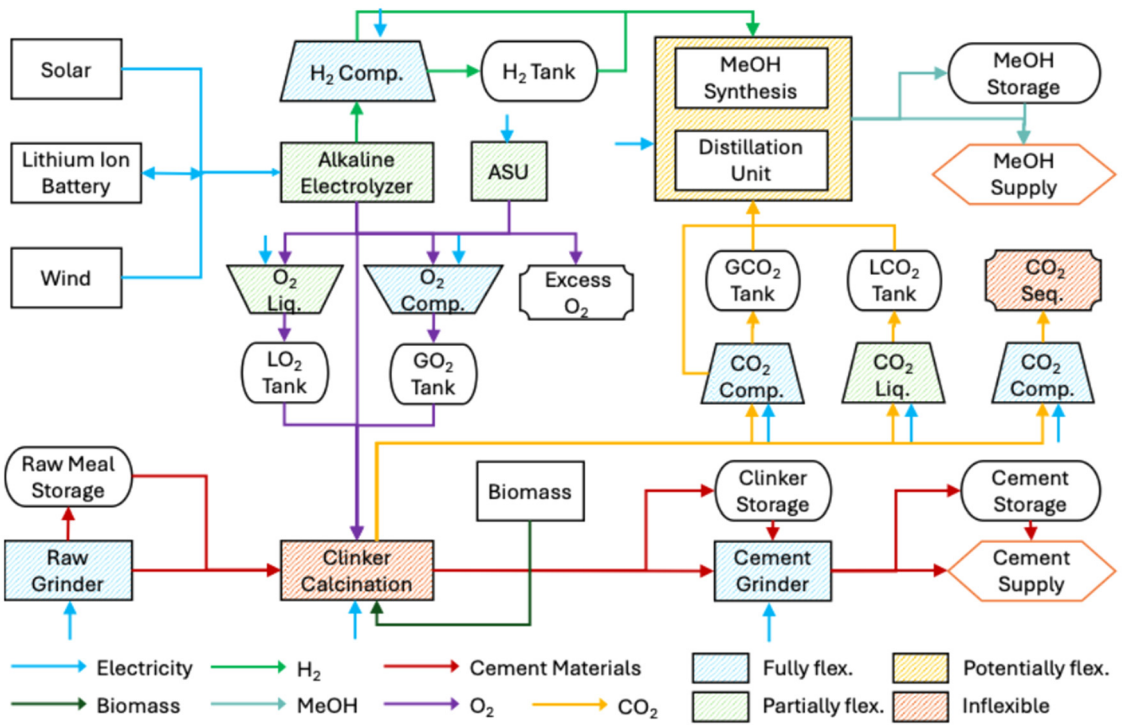

Fig. 7 Framework of the co-production system. The system is powered by solar, wind, and biomass, with all components optimized for capacity sizing and hourly operations. Storage systems for electricity, H_2, O_2, CO_2, methanol, and cement-related materials are modeled to support asynchronous operations and balance the temporal mismatch of supply and demand. Four levels of operational flexibility are defined: fully flexible (rapid response across full load with current technologies), partially flexible (response within a limited load range or subject to ramping constraints), potentially flexible (limited flexibility under current technologies but with future potential), and inflexible (constrained by inherent technical limitations). Cement and methanol supply are exogenously fixed on an hourly basis.

4.5.1. Input data preparation. The construction cost of CO_2 pipelines varies across regions due to geographic, topographic, and demographic factors. Our previous study on CO_2 source–sink matching in China's steel sector developed a geographic information system (GIS)-based cost surface with a 240 × 240 m resolution for pipeline construction.[34] In this study, we update the geographical coordinates of CO_2 sinks from prior research by incorporating new basins (see Section 6 in the SI). For CO_2 sources, we primarily evaluate the net-zero scenario by adopting the co-production strategy and compare it with the cement decarbonization-only scenario. The cement decarbonization-only scenario involves implementing CCS technology at selected cement plants without additional decarbonization measures (*e.g.*, fuel switching, efficiency improvements), while achieving the same level of CO_2 sequestration as the net-zero scenario. Under the net-zero scenario, we derive plant-level CO_2 emissions and co-production costs (excluding CO_2 transport and storage) from the process-detailed optimization model. In the cement decarbonization-only scenario, capturable CO_2 emissions at the plant level are assumed to be proportional to plant capacity, with cement production costs per tonne remaining constant (see Section 7 in the SI).

SimCCS is a decision-support software designed for the optimization and integration of CCUS technologies. One version of SimCCS generates the optimal pipeline layout under specified CO_2 sequestration targets. The input data includes geographical coordinates of CO_2 sinks and sources, the capturable CO_2 amount and capture costs by source, the sequestrable CO_2 amount and sequestration costs by sink, and the pipeline construction cost surface. The objective function minimizes the whole process cost, including capture, transport infrastructure, and sequestration costs, as defined in eqn (1), where i denotes the CO_2 source adopting CCS, and j represents the CO_2 sink utilized.

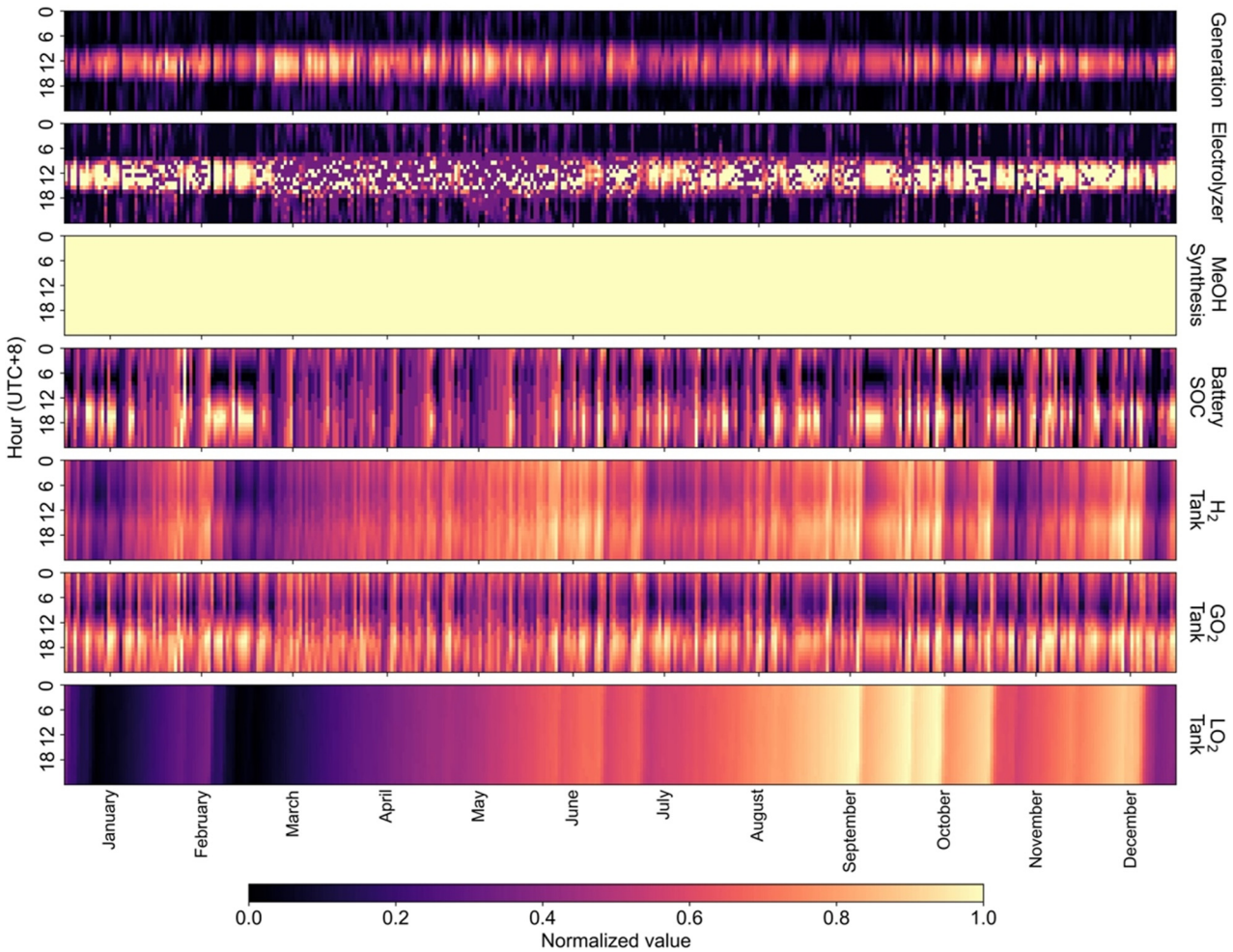

Fig. 8 Annual normalized operational profiles of the selected plant in Inner Mongolia under the net-zero cement & methanol and inflexible methanol synthesis scenario. The *x*-axis represents 365 days over one year, and the heat maps illustrate hourly variations, with the *y*-axis indicating 24 hours per day. Values are normalized by dividing hourly absolute values by their annual maximum (linear normalization). "Generation" denotes the actual hourly power generation from solar and wind, normalized by the weather-dependent maximum available hourly generation. "Electrolyzer" and "MeOH synthesis" indicate hourly loads normalized by their respective maximum loads. "State of charge (SOC)" for battery, H_2 tank, gaseous O_2 (GO_2) tank, and liquid O_2 (LO_2) tank refers to the hourly SOC normalized by each component's maximum SOC over the entire year.

In this study, we extend the SimCCS-China framework to optimize the overall CO_2 processing costs (equivalent to minimizing the CO_2 abatement cost) under predefined targets. The objective function in eqn (2) replaces the capture cost in eqn (1) with the

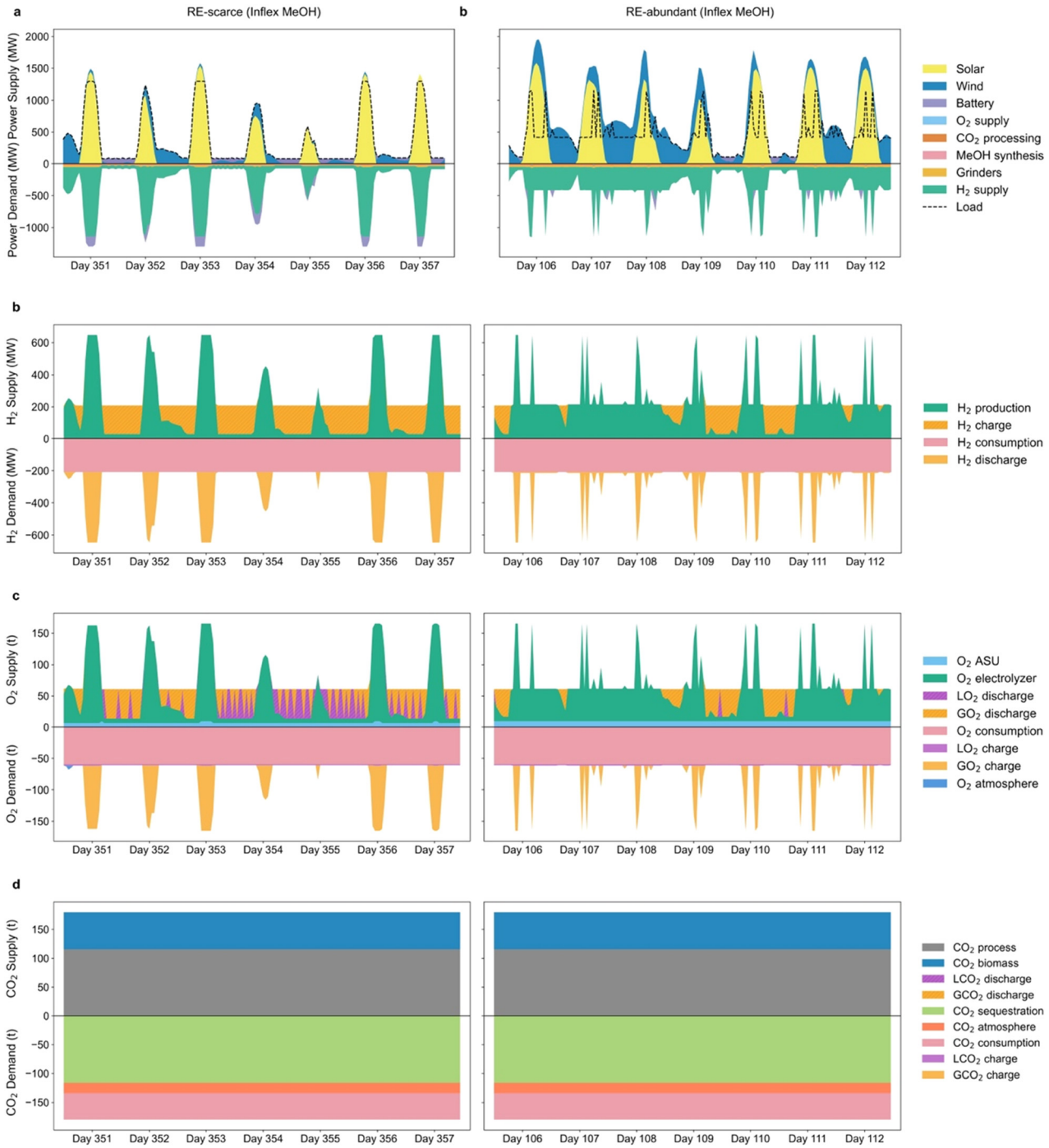

Fig. 9 Operational profiles under renewable energy (RE)-scarce and RE-abundant weeks for the selected plant in Inner Mongolia under the net-zero cement & methanol and inflexible methanol synthesis scenario. The left panels illustrate operations during a representative RE-scarce week, while the right panels show a representative RE-abundant week. In each subfigure, positive values (above the *x*-axis) indicate the supply (including discharge) of each commodity, while negative values (below the *x*-axis) indicate demand (including charge). (a) Electricity balance. The dashed line indicates the aggregated electricity load; power generation exceeding the load is curtailed. "O_2 supply" includes electricity consumed by the ASU, compressors, and liquefaction units. "CO_2 processing" includes electricity consumed by compressors and liquefaction units. "H_2 supply" represents electricity consumption for water electrolysis and H_2 compression. (b) H_2 balance. (c) O_2 balance; "O_2 atmosphere" indicates discarded O_2. (d) CO_2 balance; "CO_2 process" indicates CO_2 from carbonate decomposition, "CO_2 biogenic" indicates CO_2 from biomass combustion, and "CO_2 atmosphere" refers to CO_2 emitted to the atmosphere due to less than 100% capture rate.

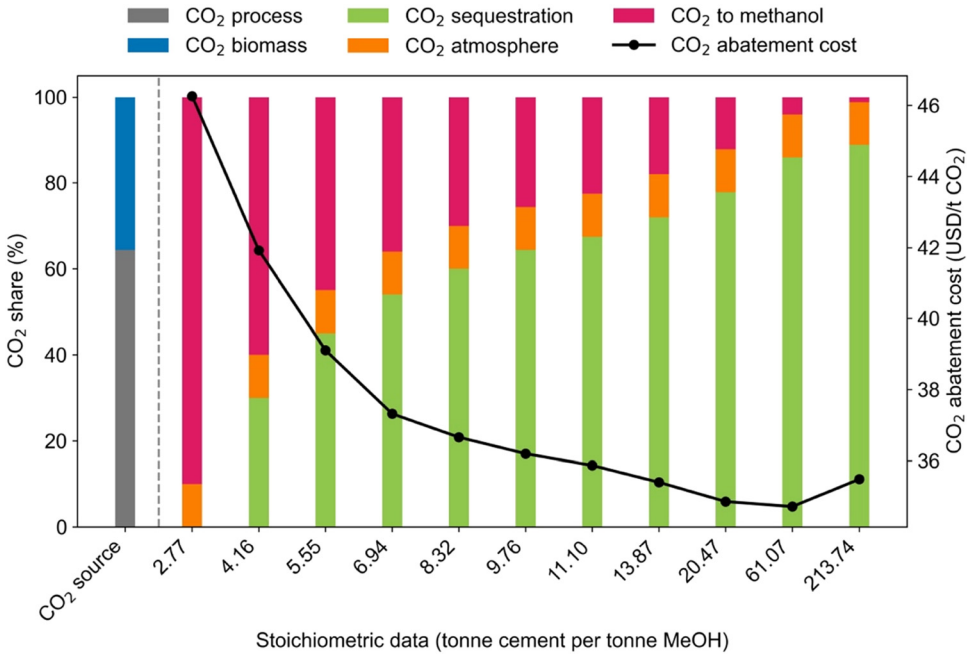

Fig. 10 CO_2 abatement cost and CO_2 share under different cement-to-methanol stoichiometric data. The leftmost bar shows the composition of the CO_2 source—exclusively from cement facilities—which remains the same across all scenarios. The subsequent bars indicate the share of CO_2 delivered to each final destination for the stoichiometric datasets on the *x*-axis. The line with markers represents the CO_2 abatement cost, calculated assuming CO_2 transport and storage costs of \$8.7 and \$5.8 per tonne of CO_2, respectively. As the ratio increases, CO_2 sequestration rises while CO_2 used for methanol synthesis correspondingly falls. This shift drives the CO_2 abatement cost down from \$46 per tCO_2 in the no-sequestration scenario to \$36 per tCO_2 under the net-zero methanol scenario (stoichiometric ratio = 9.76). Although abatement costs are minimized at stoichiometric ratios between 20.5 and 213.7, the incremental reduction relative to the net-zero methanol scenario (ratio = 9.76) is limited.

equivalent capture cost, which is derived by converting the co-production cost into an equivalent cost per unit of CO_2 sequestered (eqn (3)). At the optimum, the co-production cost, minus the cost of the coal-based benchmark technology and divided by the amount of CO_2 avoided, yields the system-level CO_2 abatement cost. We set different scales of green methanol output and convert these targets into CO_2 sequestration requirements based on the stoichiometric relationship between utilized and sequestered CO_2. Without considering CO_2 transport and sequestration costs, the co-production system is naturally favored in regions with abundant renewable energy. We incorporate post-capture (*i.e.*, transportation and storage) costs into the optimization to evaluate their impact on cost distribution and plant siting, and perform a geospatial assessment of CO_2 sequestration resources to enable source–sink matching for net-zero methanol and cement production.

$$\min \sum_{i,j} \left(\text{Capture\_cost}_i + \text{Pipeline\_cost}_{i,j} + \text{Sequestration\_cost}_j\right) \tag{1}$$

$$\min \sum_{i,j} \left(\text{Eq.capture\_cost}_i + \text{Pipeline\_cost}_{i,j} + \text{Sequestration\_cost}_j\right) \tag{2}$$

$$\begin{aligned}&\text{Eq.capture\_cost}(\$ \text{ per } tCO_2)\\ &= \text{co-production cost}(\$ \text{ per } (\text{t MeOH} + x\text{t cement}))/\text{stoichiometry}(x)/CO_2 \text{ sequestration factor}(tCO_2/\text{t cement})\end{aligned} \tag{3}$$

Author contributions

Y. H., H. L., P. L. and J. D. J. conceptualized the study and methodology. Y. H., H. L. and C. T. implemented the software, validated the model and analyzed the data, with contributions from Y. L. and Z. W. on data curation and visualization. Y. H. and Y. L. wrote the original draft, with major revisions from E. L., A. L., P. L., J. D. J., H. L., Y. F. and Z. L. E. L. and Z. L. acquired the funding. Z. L., P. L., E. L. and J. D. J. supervised the study.

Conflicts of interest

J. D. J. serves on the advisory boards of Eavor Technologies Inc., a closed-loop geothermal technology company, Rondo Energy, a provider of high-temperature thermal energy storage and industrial decarbonization solutions, Dig Energy, a developer of low-cost drilling solutions for ground-source heat pumps, and Karman Industries, a developer of advanced heat pumps for industrial applications and has an equity interest in each company. He also serves as a technical advisor to MUUS Climate Partners and Energy Impact Partners, both investors in early-stage climate technology companies.

Data availability

The data supporting this article have been included as part of the supplementary information (SI). Supplementary information is available. See DOI: https://doi.org/10.1039/d5ee07379k.

Appendix

Fig. 7–10 show the co-production framework, operational profiles under inflexible methanol synthesis, and CO_2 abatement cost and share.

Acknowledgements

The authors gratefully acknowledge the support provided by the Saudi Aramco-Tsinghua University cooperative project, Princeton University's Carbon Mitigation Initiative and the Andlinger Center for Energy and the Environment.

References

1 Intergovernmental Panel on Climate Change, *Climate Change 2022: Mitigation of Climate Change*, 2022. https://www.ipcc.ch/report/ar6/wg3/.
2 X. Yang, C. P. Nielsen, S. Song and M. B. McElroy, Breaking the hard-to-abate bottleneck in China's path to carbon neutrality with clean hydrogen, *Nat. Energy*, 2022, **7**, 955–965.
3 S. Paltsev, J. Morris, H. Kheshgi and H. Herzog, Hard-to-Abate Sectors: The role of industrial carbon capture and storage (CCS) in emission mitigation, *Appl. Energy*, 2021, **300**, 117322.
4 European Commission, Implementing the REPowerEU Action Plan: Investment Needs, Hydrogen Accelerator and Achieving the Bio-Methane Targets, 2022.
5 European Commission, Regulation (EU) 2024/1735 of the European Parliament and of the Council of 13 June 2024 on Establishing a Framework of Measures for Strengthening Europe's Net-Zero Technology Manufacturing Ecosystem and Amending Regulation (EU) *2018/1724*, 2024.
6 A. Odenweller and F. Ueckerdt, The green hydrogen ambition and implementation gap, *Nat. Energy*, 2025, **10**, 110–123.
7 T. Kazlou, A. Cherp and J. Jewell, Feasible deployment of carbon capture and storage and the requirements of climate targets, *Nat. Clim. Change*, 2024, **14**, 1047–1055.
8 M. R. Chertow, Industrial symbiosis: Literature and Taxonomy, *Annu. Rev. Energy Environ.*, 2000, **25**, 313–337.
9 Y. Kikuchi, Y. Kanematsu, M. Ugo, Y. Hamada and T. Okubo, Industrial Symbiosis Centered on a Regional Cogeneration Power Plant Utilizing Available Local Resources: A Case Study of Tanegashima, *J. Ind. Ecol.*, 2016, **20**, 276–288.
10 B. Amara, D. Kocaefe and Y. Kocaefe, A review of the studies on the utilization of petroleum pitch and its blends with coal tar pitch for carbon anode production in aluminum industry, *Next Res.*, 2025, **2**, 100250.
11 T. Gao, T. Dai, L. Shen and L. Jiang, Benefits of using steel slag in cement clinker production for environmental conservation and economic revenue generation, *J. Cleaner Prod.*, 2021, **282**, 124538.
12 M. Rehfeldt, T. Fleiter and F. Toro, A bottom-up estimation of the heating and cooling demand in European industry, *Energy Effic.*, 2018, **11**, 1057–1082.
13 International Energy Agency. Cement, IEA, 2023. https://www.iea.org/energy-system/industry/cement.
14 International Energy Agency. Chemicals, IEA, 2023. https://www.iea.org/energy-system/industry/chemicals.
15 Y. Wang, *et al.*, Historical trend and decarbonization pathway of China's cement industry: A literature review, *Sci. Total Environ.*, 2023, **891**, 164580.
16 Statista, Global methanol supply share by region, Distribution of methanol supply worldwide in 2020, by region https://www.statista.com/statistics/1323622/distribution-of-methanol-supply-worldwide-by-region/?utm_source=chatgpt.com.
17 O. Cavalett, M. D. B. Watanabe, M. Voldsund, S. Roussanaly and F. Cherubini, Paving the way for sustainable decarbonization of the European cement industry, *Nat. Sustainable*, 2024, **7**, 568–580.
18 N. de Fournas and M. Wei, Techno-economic assessment of renewable methanol from biomass gasification and PEM electrolysis for decarbonization of the maritime sector in California, *Energy Convers. Manage.*, 2022, **257**, 115440.
19 I. Servin-Balderas, K. Wetser, C. Buisman and B. Hamelers, Implications in the production of defossilized methanol: A study on carbon sources, *J. Environ. Manage.*, 2024, **354**, 120304.
20 Global CCS Institute. China begins operations at the world's largest oxy-fuel combustion CCUS project in cement sector, Global CCS Institute, 2024. https://www.globalccsinstitute.com/news-media/insights/china-begins-operations-at-the-worlds-largest-oxy-fuel-combustion-ccus-project-in-cement-sector/.
21 N. H. Prevljak, China's first full-cycle commercial green methanol project is operational, Offshore Energy, 2025. https://www.offshore-energy.biz/chinas-first-full-cycle-commercial-green-methanol-project-is-operational/.
22 Zhejiang Geely Holding Group. Inner Mongolia Alxa League 500 000-ton Green Methanol Project Kicks Off, Media Center - Zhejiang Geely Holding Group, 2024. https://zgh.com/media-center/news/2024-10-27/?lang=en.
23 F. Magli, M. Spinelli, M. Fantini, M. C. Romano and M. Gatti, Techno-economic optimization and off-design analysis of CO2 purification units for cement plants with oxyfuel-based CO_2 capture, *Int. J. Greenhouse Gas Control*, 2022, **115**, 103591.
24 Y. Mao, K. Li, J. Li, X. Zhang and J.-L. Fan, Spatial Heterogeneity of Plant-Level CCUS Investment Decisions in China's Cement Industry Under Various Policy Incentives, *Earth's Future*, 2025, **13**, e2024EF004951.
25 G. J. Fulham, P. V. Mendoza-Moreno and E. J. Marek, Managing intermittency of renewable power in sustainable

production of methanol, coupled with direct air capture, *Energy Environ. Sci.*, 2024, **17**, 4594–4621.
26 M. Fasihi and C. Breyer, Global production potential of green methanol based on variable renewable electricity, *Energy Environ. Sci.*, 2024, **17**, 3503–3522.
27 IEAGHG, Deployment of CCS in the Cement Industry, 2013. https://ieaghg.org/publications/deployment-of-ccs-in-the-cement-industry/.
28 M. Rumayor, J. Fernández-González, A. Domínguez-Ramos and A. Irabien, Deep Decarbonization of the Cement Sector: A Prospective Environmental Assessment of CO2 Recycling to Methanol, *ACS Sustainable Chem. Eng.*, 2022, **10**, 267–278.
29 Y. Wang, M. Yang, F. Shen, M. Zhou and W. Du, Conceptual design and life-cycle environmental and economic assessment of low-carbon cement manufacturing processes, *J. Cleaner Prod.*, 2024, **471**, 143349.
30 F. Williams, A. Yang and D. R. Nhuchhen, Decarbonisation pathways of the cement production process via hydrogen and oxy-combustion, *Energy Convers. Manage.*, 2024, **300**, 117931.
31 Y. He, Z. Li and P. Liu, A Co-production system of cement and methanol: Unveiling its advancements and potential, *J. Cleaner Prod.*, 2024, **473**, 143523.
32 Y. Li, Y. Li and Z. Zeng, Flexible Industrial Load Control for Renewable Power System Operation, in *Flexible Load Control for Enhancing Renewable Power System Operation*, ed. Y. Li, Y. Li and Z. Zeng, pp. 99–122, Springer Nature, Singapore, 2024, DOI: 10.1007/978-981-97-0312-8_5.
33 R. Heffron, M.-F. Körner, J. Wagner, M. Weibelzahl and G. Fridgen, Industrial demand-side flexibility: A key element of a just energy transition and industrial development, *Appl. Energy*, 2020, **269**, 115026.
34 Y. Lin, *et al.*, A preliminary assessment of CO2 capture, transport, and storage network for China's steel sector, *J. Cleaner Prod.*, 2024, **454**, 142280.
35 B. Cai, Q. Li and X. Zhang, China Status of CO_2 Capture, Utilization and Storage (CCUS) 2021 — China's CCUS Pathways, 2021. https://www.cityghg.com/file/jflyfox/cityghg/ueditor/file/20221016/20221016_215732_401737.pdf.
36 O. Schmidt, S. Melchior, A. Hawkes and I. Staffell, Projecting the Future Levelized Cost of Electricity Storage Technologies, *Joule*, 2019, **3**, 81–100.
37 M. Ren, *et al.*, Negative emission technology is key to decarbonizing China's cement industry, *Appl. Energy*, 2023, **329**, 120254.
38 T. Wu, S. T. Ng and J. Chen, Incorporating carbon capture and storage in decarbonizing China's cement sector, *Renewable Sustainable Energy Rev.*, 2025, **209**, 115098.
39 RMI, Transforming China's Chemicals Industry: Pathways and Outlook under the Carbon Neutrality Goal, 2022. https://rmi.org/insight/transforming-chinas-chemicals-industry/.
40 Y. Zhang, L. Qi, X. Lin, H. Pan and B. Sharp, Synergistic effect of carbon ETS and carbon tax under China's peak emission target: A dynamic CGE analysis, *Sci. Total Environ.*, 2022, **825**, 154076.
41 R. T. Shafiee and D. P. Schrag, Carbon abatement costs of green hydrogen across end-use sectors, *Joule*, 2024, **8**, 3281–3289.
42 A. Yagmur Goren, I. Dincer and A. Khalvati, A comprehensive review on environmental and economic impacts of hydrogen production from traditional and cleaner resources, *J. Environ. Chem. Eng.*, 2023, **11**, 111187.
43 J. Rojas, *et al.*, Technoeconomics and carbon footprint of hydrogen production, *Int. J. Hydrogen Energy*, 2024, **49**, 59–74.
44 P. Rao and M. Muller, Industrial Oxygen: Its Generation and Use. in (2007).
45 F. Eckl, A. Moita, R. Castro and R. C. Neto, Valorization of the by-product oxygen from green hydrogen production: A review, *Appl. Energy*, 2025, **378**, 124817.
46 L. Jan Müller, *et al.*, The carbon footprint of the carbon feedstock CO 2, *Energy Environ. Sci.*, 2020, **13**, 2979–2992.
47 H. Lange, A. Klose, W. Lippmann and L. Urbas, Technical evaluation of the flexibility of water electrolysis systems to increase energy flexibility: a review, *Int. J. Hydrogen Energy*, 2023, **48**, 15771–15783.
48 V. Dieterich, A. Buttler, A. Hanel, H. Spliethoff and S. Fendt, Power-to-liquid via synthesis of methanol, DME or fischer–tropsch-fuels: a review, *Energy Environ. Sci.*, 2020, **13**, 3207–3252.
49 V. A. Martinez Lopez, H. Ziar, J. W. Haverkort, M. Zeman and O. Isabella, Dynamic operation of water electrolyzers: a review for applications in photovoltaic systems integration, *Renewable Sustainable Energy Rev.*, 2023, **182**, 113407.
50 National Bureau of Statistics of China, *China Statistical Yearbook 2021*, China Statistics Press, Beijing, 2021.
51 Y. Wang, Z. Wen, M. Xu and V. Kosajan, The carbon-energy-water nexus of the carbon capture, utilization, and storage technology deployment schemes: A case study in China's cement industry, *Appl. Energy*, 2024, **362**, 122991.
52 Y. Li, S. Lan, M. Ryberg, J. Pérez-Ramírez and X. Wang, A quantitative roadmap for China towards carbon neutrality in 2060 using methanol and ammonia as energy carriers, *iScience*, 2021, **24**, 102513.
53 M. Pisciotta, *et al.*, Current state of industrial heating and opportunities for decarbonization, *Prog. Energy Combust. Sci.*, 2022, **91**, 100982.
54 Y. Y. Deng, *et al.*, Quantifying a realistic, worldwide wind and solar electricity supply, *Global Environ. Change*, 2015, **31**, 239–252.
55 E. S. Lora and R. V. Andrade, Biomass as energy source in Brazil, *Renewable Sustainable Energy Rev.*, 2009, **13**, 777–788.
56 International Carbon Action Partnership, EU emissions trading system (EU ETS), 2026. https://icapcarbonaction.com/en/ets/eu-emissions-trading-system-eu-ets.
57 International Carbon Action Partnership. China national ETS, 2025. https://icapcarbonaction.com/en/ets/china-national-ets.
58 S. Telschow, F. Frandsen, K. Theisen and K. Dam-Johansen, Cement Formation—A Success Story in a Black Box: High Temperature Phase Formation of Portland Cement Clinker, *Ind. Eng. Chem. Res.*, 2012, **51**, 10983–11004.
59 N. Tkachenko, *et al.*, Global database of cement production assets and upstream suppliers, *Sci Data*, 2023, **10**, 696.

